

UDC 537.533.2

*A.V. Arkhipov, S.I. Krel, M.V. Mishin, A.A. Uvarov*

St. Petersburg State Polytechnical University,  
29 Politekhnikeskaya St., St. Petersburg, 195251, Russia

## **CORRELATIONS IN FIELD ELECTRON EMISSION CURRENT FROM LOCAL SPOTS AT NANOPOROUS CARBON FILMS**

*A.B. Архипов, С.И. Крель, М.В. Мишин, А.А. Уваров*

## **КОРРЕЛЯЦИЯ ТОКОВ ПОЛЕВОЙ ЭМИССИИ ИЗ ЛОКАЛЬНЫХ УЧАСТКОВ ПЛЕНОК НАНОПОРИСТОГО УГЛЕРОДА**

Heterogeneous nanocarbon materials including both diamond and graphite phase domains demonstrate enhanced efficiency of electron emission that often remains unexplained by theory. Characteristic features of the actual mechanism of facilitated emission were searched for via position-resolved investigation of emission current fluctuations. The reported studies were performed with nanoporous carbon chemically derived from SiC. Partially ordered and spatially correlated character of fluctuations observed in the experiment allows to presume involvement of self-sustaining non-stationary electric field as a possible factor of emission enhancement.

FIELD-INDUCED ELECTRON EMISSION, NANOPOROUS CARBON, CORRELATION ANALYSIS.

Наноматериалы, содержащие углерод как в алмазоподобном, так и в графитоподобном состоянии, зачастую демонстрируют остающуюся пока не вполне объясненной способность к эффективной полевой эмиссии электронов. Для уточнения механизма эмиссии, реализующегося для таких материалов, мы исследовали флуктуации эмиссионных токов с высоким пространственным разрешением. Объектом исследования служили образцы нанопористого углерода, полученного химической обработкой SiC. Наблюдавшийся в экспериментах частично упорядоченный и пространственно коррелированный характер токовых флуктуаций позволяет предположить, что одним из факторов увеличения эмиссионной эффективности может служить присутствие самоподдерживающегося нестационарного электрического поля.

АВТОЭЛЕКТРОННАЯ ЭМИССИЯ, НАНОПОРИСТЫЙ УГЛЕРОД, КОРРЕЛЯЦИОННЫЙ АНАЛИЗ.

### **I. Introduction**

High efficiency of electron emission from nanocarbon materials comprised of low-aspect-ratio particles remains unexplained [1 – 5]. In many cases, the measured emission current greatly exceeded Fowler – Nordheim (FN) law predictions based on known surface morphology and electron structure. In previous works [6, 7],

we studied special features of current hysteresis in  $\mu\text{s}$ -length pulsed field regime for emitters of this type. Those experimental results allowed proposing a model of two-stage mechanism of emission: accumulation of electrons at «shallow» surface energy states under the effect of nonstationary field at the pulse front and their facilitated transition from these states

to vacuum. Our present research is aimed to investigate whether a similar mechanism can be responsible for enhanced emission in the case of constant extracting field. Even in this regime, the emission process can be affected (stimulated) by nonstationary field component associated with local fluctuations of current. On the other hand, the increased level of fluctuations in the system can be sustained by field interaction between active centers of emission. Thus, high efficiency of emission from nanocarbons in this scenario is maintained as a result of dynamic processes (auto-oscillations) developing in the emitter.

This paper presents early results of experimental study of fluctuations of emission current distribution, performed to examine the role of self-maintaining nonstationary field component in the actual emission mechanism. If this role is negligible and the emission process complies in general with FN model, fluctuations of current density measured in different emitter areas are expected to be purely statistical and independent. In the contrary case, we will observe fluctuations associated with a dynamic process. Most probably, they will be (at least, partially) ordered and correlated. Experimental definition of quantitative parameters of such an ordered oscillatory state (peak frequencies, correlation lag times, etc.) can also give new information on the nature and interaction of emission centers.

## II. Experimental Setup and Techniques

The described experiments were performed with nanocarbon film samples of the type used in previous studies [5 – 7], comprised of  $\mu\text{m}$ -size grains of nanoporous carbon (NPC). This material represents a derivative of SiC produced by chemical removal of silicon atoms (manufacturer – RSC «Applied Chemistry», St. Petersburg; for more details, see Ref. [5]). An NPC powder sample at a niobium plate was fixed behind an opening in the cathode electrode of a wide (2.5 mm) quasi-planar field gap (Fig. 1). Electrons emitted from the central part of the sample were directed through an aperture in the anode onto the phosphor screen covering the end plane of an optic fiber bunch to visualize spatial distribution of the emission current. The optic bunch served to transfer the

emission image outside of vacuum chamber ( $(1 - 7) \cdot 10^{-7}$  Torr). At its atmospheric-pressure end, the light fluxes from a few elements («pixels») of the image were collected with adjustable 50  $\mu\text{m}$ -diameter single-fiber probes for analysis of fluctuations. Phosphor screen after-glow was the principle factor limiting the data channel time resolution at approximately 0.1  $\mu\text{s}$ . Though, for the frequency range of our primary interest lying below 1 MHz [6, 7], this limitation was inessential. The spatial resolution was determined by 50  $\mu\text{m}$  diameter of the optic fibers. In comparison with characteristic dimensions of nanocarbon structure, the resolved area was very large and presumably covered with more than one active emission center. Improvement of the resolution was technically possible, but would cause the corresponding reduction of the measured light fluxes magnitudes to only a few photons per sampling interval, and hence to drastic increase of the shot noise component in the spectra. This problem was especially severe because we preferred to keep the full current extracted from the whole specimen below 3  $\mu\text{A}$  (to avoid surface degradation) and investigated properties of both active emission sites and «darker» image areas. The chosen fiber cross-section provided an acceptable balance between negative statistical effects associated with light flux (current) discontinuity and the loss of data localization.

The light fluxes corresponding to 2 or 4 selected pixels of emission image were converted, with a set of photomultipliers, into electric signals and digitized as 2048- or 4096-point oscillograms with the sampling step of 0.1 – 1.6  $\mu\text{s}$ . A typical data series measure for a fixed regime and probe positions consisted of 100 of such waveform sets. For each series, various statistical distributions were calculated, including functions of self- and cross-correlation, individual and series-averaged frequency spectra. In the case of purely statistical or chaotic fluctuations (such as « $1/f$ » or shot noise), all these functions are expected to be uniform. Any statistically significant deviations from uniformity (prominent peaks in spectra, intervals of temporary regularization in waveforms, delayed cross-correlation between signals, etc.) were noted as signs of ordering.

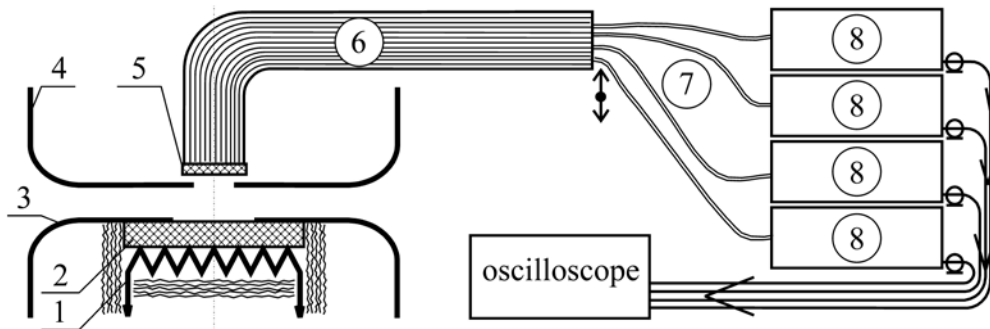


Fig. 1. Experimental setup scheme:

1 – cathode heater; 2 – emitter sample; 3 – cathode cover; 4 – anode; 5 – phosphor screen; 6 – evacuated optic bunch; 7 – light-guide fiber probes; 8 – photomultipliers  
Field gap width is 2.5 mm, openings in the cathode cover and in the anode are 6 and 2 mm in diameter respectively

### III. Emission Image Structure and Dynamics

The tested nanocarbon samples demonstrated moderate emission efficiency: 1  $\mu\text{A}$  current was achieved at 12 – 16 kV gap voltage, which corresponds to mean field magnitude 4.8 – 6.4 V/ $\mu\text{m}$ . Examined under a microscope, a typical low-current emission pattern was comprised of bright spots of 200 – 400  $\mu\text{m}$  in size with darker intervals between them. The natural assumption that each spot represents a smeared image of a single emission center proved to be wrong, because different pixels belonging to the same spot demonstrated relatively independent behavior in time – they flickered and even «turned off» and «on» separately. Positions of the probe fibers were chosen so as to compare light flux fluctuations for the pixels belonging to different parts of the same spot, or to different spots.

### IV. Statistical Properties of Local Emission Waveforms

The measured current density fluctuation data can be roughly divided, in accordance with their statistical properties, into two major groups.

For relatively low-current-density parts of the emitting pattern, such as peripheral pixels surrounding the bright spots, signals with dominating low-frequency spectral components were most typical. The spectra averaged over a data series (100 waveforms) were very smooth, and either had a broad maximum near 30 – 50 kHz (see Probe 1 plot in Fig. 2) or were « $1/f$ » type. Individual signal waveforms often represented successions of microsecond-length photon bunches separated by irregular gap time intervals (Fig. 3). In this case, insta-

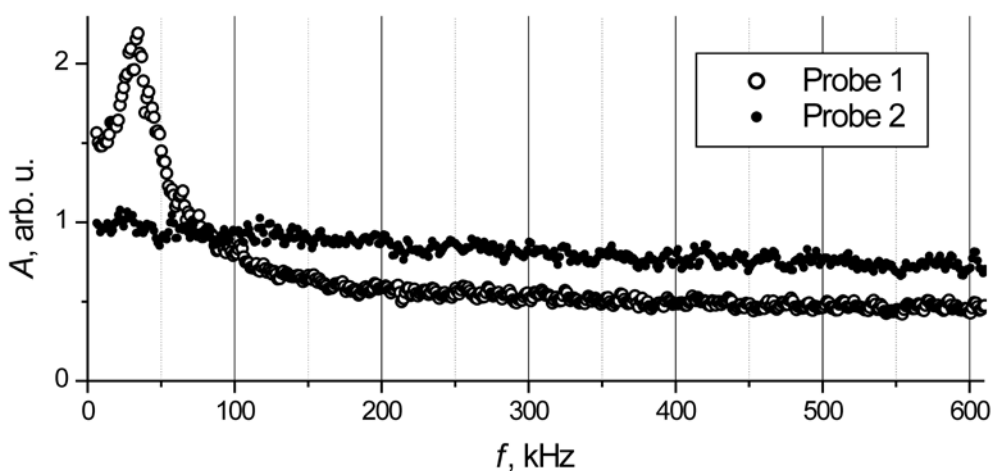


Fig. 2. Series-averaged frequency spectra for two pixels of emission image spaced by 150  $\mu\text{m}$ . Probe 1 is placed near the center of a bright spot, probe 2 – in its peripheral part

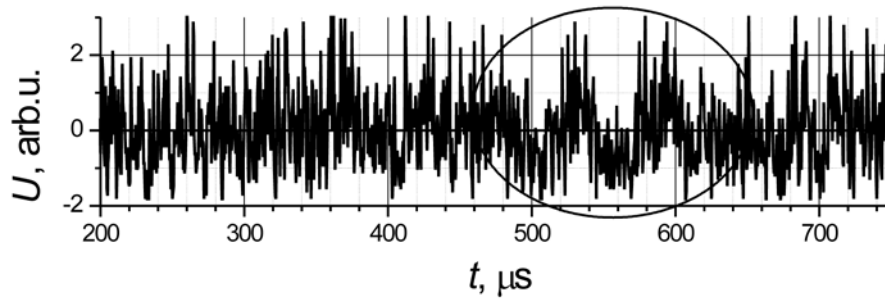


Fig. 3. A typical emission signal waveform with an interval of partial regularization

bility of emission process and dynamical character of its fluctuations are apparent.

For the brighter parts of the emission pattern, averaged frequency characteristics of fluctuation signals usually were practically uniform all over the surveyed range (Probe 2 in Fig. 2). The corresponding waveforms were visibly chaotic over the main part of their lengths, yet occasionally included intervals of more regular behavior – such as the one presented in Fig. 4. During these intervals, quasi-periodic modulation grew simultaneously with reduction of the noise-like component, so that the full energy of the signal remained approximately constant. This feature proves that even when

the observed fluctuations are disordered, they have dynamic nature – because the basic statistical noise cannot be suppressed by interference with an ordered signal.

### V. Cross-Correlation of Signals

Another notable feature of emission pattern fluctuations consisted of partial correlation of current density signals measured at different positions. No correlations of this sort were ever observed for a pair of pixels belonging to different bright spots comprising the pattern. Signals from different parts of the same spot were definitely correlated for approximately 50 % of acquired data series. Fig. 4 represents series-

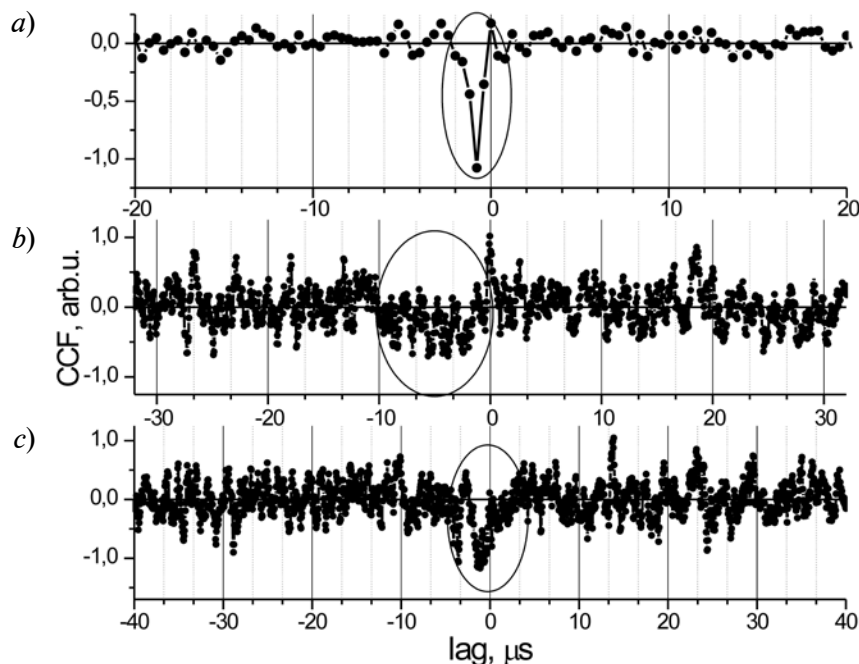


Fig. 4. Series-averaged cross-correlation functions of emission signals displaying statistically significant delayed correlation. In all cases the probe spacing is 150 μm



averaged cross-correlation function (CCF) plots for light flux signals from pixels spaced by 150  $\mu\text{m}$  distance. The upper plot illustrates the case of one-directional suppression of the weaker signal from the peripheral part of a bright spot by high-magnitude signal from the spot core with well-defined lag time close to 1  $\mu\text{s}$ . The effective peak stands far out against the background noise. Absence of zero-lag correlation allows to exclude its attribution to instrumental sources, such as light flux mixing or electric signal interference. The CCF plotted in Fig. 4, *b* gives another example of statistically significant cross-correlation, with characteristic lag times of the effect lying in much broader range between 0 and 10  $\mu\text{s}$ . Fig. 4, *c* demonstrates a case of more «symmetric» mutual suppression developing between emission pattern areas with comparable brightness. The effect is notable for the lag absolute values up to 2 – 3  $\mu\text{s}$ .

Thus, the fact of correlated behavior of field-induced current density fluctuations has been established experimentally for measurement points spaced by distances as large as 100 – 300  $\mu\text{m}$ , which can be interpreted as a sign of involvement of large continuously-active specimen areas in universal wave-like processes. The observed cross-correlation lag times suggest the wave propagation velocity

range 10 – 100 m/s. These values look too small for waves of electromagnetic and even acoustic nature, but could be explained by models based on thermal processes [8] or, for instance, electric charge transfer in weakly-conducting  $\mu\text{m}$ -grain powder. Currently, we are launching experiments with larger probe arrays to investigate this possibility in more detail and to perform a more accurate measurement of the characteristics of presumably propagating emission waves.

## VI. Conclusions

The performed experiments have demonstrated that fluctuations of field-induced emission current from an NPC layer in dc extraction regime have dynamic nature and in some cases are partially correlated for large areas of emitter surface (as much as 100 – 300  $\mu\text{m}$  in size). These properties cannot be adequately explained by any model considering the field emission from materials of the investigated type as an instant and local process. Thus, another indirect confirmation of the role of non-stationary field in emission is found. Typical periods of ordered oscillations and cross-correlation lag times observed in these experiments (1 – 10  $\mu\text{s}$ ) agree with our previous results for pulsed-field regime hysteresis [6, 7].

## REFERENCES

1. **Forbes R.G.** Field emission: New theory for the derivation of emission area from a Fowler–Nordheim plot. *Journal of Vacuum Science & Technology B: Microelectronics and Nanometer Structures*, 1999, Vol. 17, Iss. 2, pp. 526–533.
2. **Frolov V.D., Karabutov A.V., Pimenov S.M., Konov V.I.** Electronic properties of the emission sites of low-field emitting diamond films. *Diamond and Related Materials*, 2000, Vol. 9, No. 3, pp. 1196–1200.
3. **Obraztsov A.N., Pavlovskii I.Y., Volkov A.P.** Field electron emission in graphite-like films. *Technical Physics*, 2001, Vol. 46, No. 11, pp. 1437–1443.
4. **Okotrub A.V., Bulusheva L.G., Gusel'nikov A.V., Kuznetsov V.L., Butenko Y.V.** Field emission from products of nanodiamond annealing. *Carbon*, 2004, Vol. 42, No. 5, pp. 1099–1102.
5. **Bondarenko V.B., Gabdullin P.G., Gnuchev N.M., Davydov S.N., Korablev V.V., Kravchik A.E., Sokolov V.V.** Emissivity of powders prepared from nanoporous carbon. *Technical physics*, 2004, Vol. 49, No. 10, pp. 1360–1363.
6. **Arkhipov A.V., Mishin M.V., Sominski G.G., Parygin I.V.** Hysteresis of pulsed characteristics of field emission from nanocarbon films. *Technical Physics*, 2005, Vol. 50, No. 10, pp. 1353–1359.
7. **Arkhipov A.V., Mishin M.V., Parygin I.V.** Hysteresis of pulsed characteristics of field emission from nanocarbon materials. *Surface and interface analysis*, 2007, Vol. 39, No. 2–3, pp. 149–154.
8. **Vul A.Y., Eidelman E.D., Dideikin A.T.** Thermoelectric Effect in Field Electron Emission from Nanocarbon. In *Synthesis, Properties and Applications of Ultrananocrystalline Diamond*. Springer Netherlands, 2005, pp. 383–394.

## СПИСОК ЛИТЕРАТУРЫ

1. **Forbes R.G.** Field emission: New theory for the derivation of emission area from a Fowler–Nordheim plot. *Journal of Vacuum Science & Technology B: Microelectronics and Nanometer*

*Structures*, 1999, Vol. 17, Iss. 2, pp. 526–533.

2. **Frolov V.D., Karabutov A.V., Pimenov S.M., Konov V.I.** Electronic properties of the emission sites of low-field emitting diamond films. *Diamond and Related Materials*, 2000, Vol. 9, No. 3, pp. 1196–1200.

3. **Obraztsov A.N., Pavlovskii I.Y., Volkov A.P.** Field electron emission in graphite-like films. *Technical Physics*, 2001, Vol. 46, No. 11, pp. 1437–1443.

4. **Okotrub A.V., Bulusheva L.G., Gusel'nikov A.V., Kuznetsov V.L., Butenko Y.V.** Field emission from products of nanodiamond annealing. *Carbon*, 2004, Vol. 42, No. 5, pp. 1099–1102.

5. **Bondarenko V.B., Gabdullin P.G., Gnuchev N.M., Davydov S.N., Korablev V.V., Kravchik**

**A.E., Sokolov V.V.** Emissivity of powders prepared from nanoporous carbon. *Technical physics*, 2004, Vol. 49, No. 10, pp. 1360–1363.

6. **Arkhipov A.V., Mishin M.V., Sominski G.G., Parygin I.V.** Hysteresis of pulsed characteristics of field emission from nanocarbon films. *Technical Physics*, 2005, Vol. 50, No. 10, pp. 1353–1359.

7. **Arkhipov A.V., Mishin M.V., Parygin I.V.** Hysteresis of pulsed characteristics of field emission from nanocarbon materials. *Surface and interface analysis*, 2007, Vol. 39, No. 2–3, pp. 149–154.

8. **Vul A.Y., Eidelman E.D., Dideikin A.T.** Thermoelectric Effect in Field Electron Emission from Nanocarbon. In *Synthesis, Properties and Applications of Ultrananocrystalline Diamond*. Springer Netherlands, 2005, pp. 383–394.

---

**АРХИПОВ Александр Викторович** – кандидат физико-математических наук, доцент кафедры физической электроники Санкт-Петербургского государственного политехнического университета.

195251, Россия, Санкт-Петербург, Политехническая ул., 29  
arkhipov@rphf.spbstu.ru

**КРЕЛЬ Святослав Игоревич** – аспирант кафедры физической электроники Санкт-Петербургского государственного политехнического университета.

195251, Россия, Санкт-Петербург, Политехническая ул., 29  
8svyatoslav8@mail.ru

**МИШИН Максим Валерьевич** – доцент кафедры физико-химии и технологий микросистемной техники Санкт-Петербургского государственного политехнического университета.

195251, Россия, Санкт-Петербург, Политехническая ул., 29  
max@mail.spbstu.ru

**УВАРОВ Андрей Анатольевич** – доцент кафедры физико-химии и технологий микросистемной техники Санкт-Петербургского государственного политехнического университета.

195251, Россия, Санкт-Петербург, Политехническая ул., 29